Type V Collagen Regulates the Structure and Biomechanics of TMJ Condylar Cartilage: A Fibrous-Hyaline Hybrid

Prashant Chandrasekaran , Bryan Kwok , Biao Han , Sheila M. Adams , Chao Wang , Daphney R. Chery , Robert L. Mauck , Nathaniel A. Dyment , X. Lucas Lu , David B. Frank , Eiki Koyama , David E. Birk , Lin Han

PII: S0945-053X(21)00066-4
DOI: https://doi.org/10.1016/j.matbio.2021.07.002
Reference: MATBIO 1691

To appear in: *Matrix Biology*

Received date: 14 October 2020
Revised date: 26 May 2021
Accepted date: 15 July 2021

Please cite this article as: Prashant Chandrasekaran , Bryan Kwok , Biao Han , Sheila M. Adams , Chao Wang , Daphney R. Chery , Robert L. Mauck , Nathaniel A. Dyment , X. Lucas Lu , David B. Frank , Eiki Koyama , David E. Birk , Lin Han , Type V Collagen Regulates the Structure and Biomechanics of TMJ Condylar Cartilage: A Fibrous-Hyaline Hybrid, *Matrix Biology* (2021), doi: https://doi.org/10.1016/j.matbio.2021.07.002

Highlights

- Type V collagen regulates the collagen fibril nanostructure and micromechanics of both the fibrocartilage and hyaline cartilage layers in temporomandibular joint condyle.
- Reduction of type V collagen leads to decreased cell density and aberrant cell clustering in both fibrous and hyaline layers.
- Loss of type V collagen leads to reduced cell proliferation and β-catenin expression in the fibrous layer, indicating its role in maintaining the progenitor cell niche in condylar cartilage.
- Ablation of type V collagen at the post-weaning age results in pronounced thinning of the hyaline layer, highlighting the interplay between type V collagen and mechanoregulation of condylar cartilage growth.
- The role of type V collagen in regulating cell fate is specific to the progenitor cells in condylar cartilage, and is absent in knee cartilage.

Type V Collagen Regulates the Structure and Biomechanics of TMJ Condylar Cartilage: A Fibrous-Hyaline Hybrid

Prashant Chandrasekaran[a], *Bryan Kwok*[a], *Biao Han*[a], *Sheila M. Adams*[b], *Chao Wang*[a], *Daphney R. Chery*[a], *Robert L. Mauck*[c,d], *Nathaniel A. Dyment*[c], *X. Lucas Lu*[e], *David B. Frank*[f,g,h], *Eiki Koyama*[i], *David E. Birk*[b], *Lin Han*[a,*]

[a]School of Biomedical Engineering, Science and Health Systems, Drexel University, Philadelphia, PA 19104, United States

[b]Department of Molecular Pharmacology and Physiology, Morsani School of Medicine, University of South Florida, Tampa, FL 33612, United States

[c]McKay Orthopaedic Research Laboratory, Department of Orthopaedic Surgery, Perelman School of Medicine, University of Pennsylvania, Philadelphia, PA 19104, United States

[d]Translational Musculoskeletal Research Center, Corporal Michael J. Crescenz Veterans Administration Medical Center, Philadelphia, PA 19104, United States

[e]Department of Mechanical Engineering, University of Delaware, Newark, DE 19716, United States

[f]Penn-CHOP Lung Biology Institute, Perelman School of Medicine, University of Pennsylvania, Philadelphia, PA 19104, United States

[g]Penn Cardiovascular Institute, Perelman School of Medicine, University of Pennsylvania, Philadelphia, PA 19104, United States

[h]Division of Pediatric Cardiology, Department of Pediatrics, The Children's Hospital of Philadelphia, Philadelphia, PA 19104, United States

[i]Translational Research Program in Pediatric Orthopaedics, Division of Orthopaedic Surgery, The Children's Hospital of Philadelphia, Philadelphia, PA 19104, United States

*Correspondence and requests for materials should be addressed to:

Dr. Lin Han
Phone: (215) 571-3821
Fax: (215) 895-4983
Email: lh535@drexel.edu.

For submission to *Matrix Biology* as a *Regular Research Paper*.

Abstract

This study queried the role of type V collagen in the post-natal growth of temporomandibular joint (TMJ) condylar cartilage, a hybrid tissue with a fibrocartilage layer covering a secondary hyaline cartilage layer. Integrating outcomes from histology, immunofluorescence imaging, electron microscopy and atomic force microscopy-based nanomechanical tests, we elucidated the impact of type V collagen reduction on TMJ condylar cartilage growth in the type V collagen haploinsufficiency and inducible knockout mice. Reduction of type V collagen led to significantly thickened collagen fibrils, decreased tissue modulus, reduced cell density and aberrant cell clustering in both the fibrous and hyaline layers. Post-natal growth of condylar cartilage involves the chondrogenesis of progenitor cells residing in the fibrous layer, which gives rise to the secondary hyaline layer. Loss of type V collagen resulted in reduced proliferation of these cells, suggesting a possible role of type V collagen in mediating the progenitor cell niche. When the knockout of type V collagen was induced in post-weaning mice after the start of physiologic TMJ loading, the hyaline layer exhibited pronounced thinning, supporting an interplay between type V collagen and occlusal loading in condylar cartilage growth. The phenotype in hyaline layer can thus be attributed to the impact of type V collagen on the mechanically regulated progenitor cell activities. In contrast, knee cartilage does not contain the progenitor cell population at post-natal stages, and develops normal structure and biomechanical properties with the loss of type V collagen. Therefore, in the TMJ, in addition to its established role in regulating the assembly of collagen I fibrils, type V collagen also impacts the mechanoregulation of progenitor cell activities in the fibrous layer. We expect such knowledge to establish a foundation for understanding condylar cartilage matrix development and regeneration, and to yield new insights into the TMJ symptoms in patients with classic Ehlers-Danlos syndrome, a genetic disease due to autosomal mutation of type V collagen.

Keywords:

Type V collagen, cartilage matrix, temporomandibular joint, mechanobiology, collagen fibrils, Ehlers-Danlos syndrome.

Introduction

Temporomandibular joint (TMJ) disorder, known as TMD, afflicts 5-12% of the US population, leading to limited jaw motion and chronic pain [1]. TMD, especially TMJ osteoarthritis, is associated with degeneration of the mandibular condylar cartilage, a pivotal unit to the load bearing and energy dissipation functions for everyday jaw activities such as speaking and chewing [2]. Successful regeneration of condylar cartilage holds the potential for restoring joint function for TMD patients without causing common complications, including bone resorption or revision surgery, from standard treatments such as prosthetics and autografts [3]. However, one major roadblock for developing effective regeneration strategy [4] is the lack of understanding of the formation and degeneration of condylar cartilage extracellular matrix (ECM) [5]. The ECM has a hybrid structure integrating a fibrocartilage layer covering a secondary hyaline cartilage layer [6, 7]. This is distinct from the articular surfaces of other diarthrodial joints that are dominated by hyaline cartilage [8]. To this day, there is little knowledge on the molecular activities that govern the formation of this unique hybrid ECM. Establishing the structure-mechanics principles of condylar cartilage ECM will provide the necessary benchmark for designing regenerative strategies [9]. Furthermore, the integrity of ECM is pivotal to cell mechanotransduction, and aberrant remodeling of the ECM is a major driving force of tissue dysfunction and perturbed cell signaling in disease [10-12]. Understanding the activities of ECM molecules will enable a more targeted design of disease intervention and regeneration strategies for this unique tissue [13, 14].

Type V collagen (collagen V) could be a central player in the establishment of condylar cartilage ECM. *In vivo*, collagen V serves as the co-nucleator for initiating collagen I fibrillogenesis [15], and its partially processed N-propeptide projects outward from the fibril

surface to limit aberrant fibril lateral growth [16]. In tension-bearing fibrous tissues such as skin [15], tendon [17] and cornea [18], reduction of collagen V leads to abnormally thickened collagen fibrils, reduced fibril numbers and impaired mechanical properties. Complete deletion of *Col5a1* gene in mice results in embryonic lethality due to the incapability of collagen I fibrillogenesis [19]. Since the top layer of TMJ condylar cartilage consists of collagen I-dominated fibrocartilage [6], collagen V could play an essential role in regulating the formation and maintenance of this layer. In fact, the importance of collagen V to TMJ health is highlighted by the higher propensity towards TMD in patients with classic Ehlers-Danlos syndrome (cEDS) [20], a human autosomal dominant disorder (prevalence of ~ 1:20,000) due to the mutation of *COL5A1* or *COL5A2* gene [21].

This study aimed to elucidate the role of collagen V in the structure and biomechanics of TMJ condylar cartilage *in vivo*. To assess the impact of collagen V deficiency on condylar cartilage ECM, we studied the murine model of cEDS ($Col5a1^{+/-}$ [15]) at 3 months of age. To determine the age-dependent impact of collagen V loss, we tested the recently established inducible collagen V knockout mice ($Col5a1^{iKO}$ [18]). In these mice, we maintained the normal level of collagen V in embryonic and neo-natal development, induced the knockout of *Col5a1* gene expression at 1 week (pre-weaning) and 1 month (post-weaning) of ages, and analyzed the resulted phenotype at 1 and 2 months of ages, respectively. We assessed condylar cartilage morphology and cellularity, major ECM molecule distribution, collagen fibril nanostructure, as well as condylar cartilage tissue modulus. In these tests, the fibrous and hyaline layers were analyzed separately to delineate the role of collagen V in these two distinct units. In addition, to determine if the observed defects of condylar cartilage are associated with tissue-specific activities of collagen V, we also tested the structure and biomechanics of knee cartilage in these

mice, and compared cell proliferation and other phenotypic changes between condylar cartilage and knee cartilage. Our findings pointed to a crucial role of collagen V in regulating both matrix assembly and mechanosensitive cell activities during the post-natal growth of condylar cartilage.

Results

Distribution of ECM molecules in TMJ condylar cartilage

To assess the distribution of collagen V in condylar cartilage, we applied immunofluorescence (IF) imaging to the condylar cartilage of 3-month-old wild-type (WT) and *Col5a1*$^{+/-}$ mice. In WT condylar cartilage, collagen V was found to be highly expressed in the fibrous layer with a preferential localization in the pericellular domain (Fig. 1a), similar to its distribution pattern in tendon [22]. In the hyaline layer, collagen V was present at much lower concentration, with trace amount detected in the pericellular region. In *Col5a1*$^{+/-}$ mice, the amount of collagen V protein was markedly reduced relative to WT, validating the reduction of collagen V in this model.

We then compared the distributions of other major ECM constituents between WT and *Col5a1*$^{+/-}$ condylar cartilage. As expected, collagen I was more concentrated in the top fibrous layer (Fig. 1b), while collagen II was localized in the hyaline layer (Fig. 1c). There was also modest amount of collagen I in the hyaline layer, which may represent collagen fibers that are originated from the fibrous layer and rooted into subchondral bone [23]. Aggrecan, the major proteoglycan of hyaline cartilage matrix, was present in both hyaline and fibrous layers, with reduced concentration near the surface (Fig. 1d). In the hyaline layer, the two biomarkers of cartilage pericellular matrix (PCM), collagen VI and perlecan [24], were localized in the PCM, as expected (Fig. 1e,f). In the fibrous layer, however, collagen VI was present throughout the

matrix, while perlecan still showed a more preferential localization in the pericellular domain. The differentiated distributions of collagen VI and perlecan were similar to their patterns in bovine meniscus [25, 26], suggesting perlecan to be a more specific biomarker of fibrocartilage PCM than collagen VI. Comparing the two genotypes, we did not notice appreciable changes in the distributions of these molecules, except for that of collagen V (Fig. 1). Therefore, reduction of collagen V did not markedly alter the major ECM constituents of the two layers, or the compositional distinction between the PCM and territorial/interterritorial extracellular matrix (T/IT-ECM) domains that are further removed from cells.

Impact of collagen V reduction on the morphology and structure of condylar cartilage

To determine the contribution of collagen V to condylar cartilage matrix integrity, we first applied histology to assess the gross-level morphology and cellularity of the TMJ in 3-month-old WT and *Col5a1*$^{+/-}$ mice. We found that reduction of collagen V did not lead to significant changes in the thicknesses of either fibrous or hyaline layers (Fig. 2a,b). We also did not detect appreciable changes in sulfated glycosaminoglycan (sGAG) staining (Fig. 2a), indicating that the formation of hyaline cartilage was not impaired at the histological level. However, in both fibrous and hyaline layers, there was a significant reduction in overall cell density (Fig. 2a,c) and increase in cell clustering (Fig. 2a, black arrowheads, and 2d), indicating possible impairment of cell proliferation associated with collagen V reduction.

We then tested the impact of collagen V reduction on the nanostructure of collagen fibrils by applying scanning electron microscopy (SEM) to the condylar surface and transmission electron microscopy (TEM) to the cross-section of matrix interior (Fig. 3 and Table 1). On the surface, there was a significant increase in average fibril diameter and variance (≥ 800 fibrils, n =

3 animals each group). In the interior, for the fibrous layer, a similar contrast was observed, where *Col5a1*$^{+/-}$ condylar cartilage exhibited increased fibril diameter and variance (Fig. 3b,c and Table 1, ≥ 350 fibrils, $n = 3$). These structural defects illustrated the established role of collagen V, which is to limit the aberrant lateral growth of collagen I fibrils [16]. With the reduction of collagen V, condylar surface maintained the transverse random fibrillar architecture (Fig. 3a). This indicates that at 3 months of age, haploinsufficiency of collagen V has not yet led to aberrant surface fibrillation, which is signified by the formation of highly aligned collagen fibers [27, 28].

In the hyaline layer, despite the relatively low concentration of collagen V therein (Fig. 1a), we also detected significant structural defects with its reduction, as illustrated by the significant increase in both fibril diameter and variance (≥ 550 fibrils, $n = 3$, Fig. 3b,c and Table 1). Thus, in condylar cartilage, collagen V influences the fibril structure of both fibrous and hyaline layers. The structural defects in the hyaline layer cannot be directly explained by the established role of collagen V [16], and could suggest new activities of collagen V in regulating the growth of condylar cartilage.

Impact of collagen V reduction on condylar cartilage biomechanics

To determine how the structural defects caused by collagen V reduction impairs the biomechanical properties of condylar cartilage, we first applied AFM-nanoindentation to measure the surface modulus of condylar cartilage in the central region. Results showed that the modulus of *Col5a1*$^{+/-}$ condylar cartilage (0.10 ± 0.05 MPa, mean ± 95% CI, $n = 7$) was 61 ± 20% (mean ± 95% CI) lower than that of WT ($p = 0.007$, 0.26 ± 0.09 MPa, $n = 7$, Fig. 4a,b). In the AFM test, the maximum indentation depth was controlled at ≈ 0.4-0.6 μm, which reflects the

mechanical properties of top ~ 4-6 μm layer (~ 10× maximum indentation depth [29]) of condylar cartilage. Given that the fibrous layer is ≈ 20 μm thick in the central region (Fig. 2b), this modulus reduction mainly reflects the impairment of fibrous layer.

To assess the modulus of hyaline layer, we applied perlecan IF-guided AFM nanomechanical mapping to the cryo-section of freshly dissected condylar cartilage, which also allows us to delineate the micromodulus of PCM and T/IT-ECM [30, 31]. In both the PCM and T/IT-ECM, we detected significantly lower modulus with the reduction of collagen V (Fig. 4c). For the PCM, the modulus of *Col5a1*$^{+/-}$ group (0.052 ± 0.014 MPa, n = 7) was 51 ± 21% lower than that of WT (0.106 ± 0.064 MPa, p = 0.010), and for the T/IT-ECM, the modulus (0.080 ± 0.027 MPa for *Col5a1*$^{+/-}$) was 59 ± 23% lower (0.184 ± 0.084 MPa for WT, p = 0.010, Fig. 4d). For both genotypes, as expected, the PCM modulus was significantly lower than the T/IT-ECM (p = 0.036 for WT, p = 0.043 for *Col5a1*$^{+/-}$). Taken together, deficiency of collagen V has a profound impact on the biomechanics of TMJ condylar cartilage, leading to the impairment of both fibrous and hyaline layers, and in both the overt tissue-level properties and microscale properties of the PCM.

Age-dependent impact of collagen V knockout on condylar cartilage post-natal growth

Next, we tested how induced post-natal ablation of collagen V impacts the growth of condylar cartilage using the *Col5a1*^{iKO} model. In these mice, we confirmed that tamoxifen injection significantly reduced *Col5a1* gene expression by quantitative PCR (Fig. 5a) and collagen V protein content by IF (Fig. 5b), validating the use of this model for studying the temporal impact of collagen V loss. We compared the TMJ phenotype in *Col5a1*^{iKO} mice at 1 and 2 months of ages, following the induced knockout at 1 week and 1 month of ages,

respectively. In both age groups, induced knockout of *Col5a1* did not alter the thicknesses of both layers at the anterior and posterior ends (Fig. 5c,d), but resulted in significant decrease in cell density (Fig. 5e), increase in cell clustering (Fig. 5f) and reduction in tissue modulus (0.126 ± 0.048 MPa for control versus 0.026 ± 0.013 MPa for $Col5a1^{iKO}$ at 1 month of age, 79 ± 4% reduction, $p = 0.002$; 0.124 ± 0.059MPa for control versus 0.032 ± 0.015 MPa for $Col5a1^{iKO}$ at 2 months of age, 74 ± 26% reduction, $p = 0.004$, Fig. 5g). These defects were similar to those observed in $Col5a1^{+/-}$ mice. Notably, there was a significant reduction of hyaline cartilage thickness in the central region ($p = 0.048$) for the 2-month group, but not the 1-month group (Fig. 5c,d). Given that the TMJ experiences higher physiologic loading after weaning at 3 weeks [32-34], such contrast indicates the activities of collagen V could vary with age and be coupled with post-weaning occlusal loading.

Absence of structural and biomechanical phenotype in knee cartilage with the reduction of collagen V

To compare the activities of collagen V in condylar cartilage versus knee cartilage, we tested the structure and biomechanics of knee cartilage in both $Col5a1^{+/-}$ and $Col5a1^{iKO}$ mice. In 3-month-old WT knee joint, collagen V was found to be present only in the pericellular domain of the top superficial layer, and absent in the middle and deep layers (Fig. 6a). Given the relative low content of collagen V, we did not detect appreciable differences between WT and $Col5a1^{+/-}$ joints, unlike the case of condylar cartilage (Fig. 1a). Also, in contrast to the pronounced defects of the T MJ, $Col5a1^{+/-}$ knee joints showed normal cartilage thickness, sGAG staining and cell density (Fig. 6b-d), and did not exhibit aberrant cell clustering as in TMJ condylar cartilage.

The surface of both WT and *Col5a1*$^{+/-}$ cartilage exhibited the transversely random fibrillar architecture, as shown by SEM (Fig. 7a). In comparison to the WT, *Col5a1*$^{+/-}$ cartilage surface had similar average fibril diameter (Fig. 7b), but contained a higher amount of both thinner and thicker fibrils, contributing to a significantly higher variance of fibril diameter (Fig. 7c). This indicates collagen V may play a role in mediating surface fibril homogeneity. On the other hand, AFM-nanoindentation yielded similar modulus between WT (1.39 ± 0.51 MPa) and *Col5a1*$^{+/-}$ (1.04 ± 0.15 MPa, $p = 0.530$) cartilage (Fig. 7d). Similarly, *Col5a1*^{iKO} knee cartilage showed normal thickness, sGAG staining and cell density, as well as absence of cell clustering, at both 1 and 2 months of ages (Fig. 8a-c). Meanwhile, AFM-nanoindentation also detected similar modulus between control and *Col5a1*^{iKO} groups (Fig. 8d). Therefore, at least in the tested age groups, reduction of collagen V did not impair the post-natal development and load-bearing biomechanical function of knee cartilage. This lack of phenotype is in stark contrast to the pronounced defects in condylar cartilage hyaline layer, pointing to a tissue-specific role of collagen V in the TMJ.

Impact of collagen V reduction on cell proliferation and β-catenin expression

Given the reduction in cell density observed in collagen V-deficient condylar cartilage, we analyzed the expression of Ki-67, the cell proliferation biomarker [35], in 1-month-old *Col5a1*^{iKO} and control mice (Fig. 9a,b). In the control mice, we detected appreciable Ki-67-positive cells in the fibrous layer, affirming the proliferative capability of progenitor cells therein. In contrast, the Ki-67 staining was absent in the underlying secondary hyaline layer, underscoring clear differences in the differentiation stages of cells within the two layers. In *Col5a1*^{iKO} condyle, the number of Ki-67-positive cells staining was significantly reduced in the fibrous layer, and was also absent in the hyaline layer. Therefore, reduction of collagen V was

found to impair the proliferation of progenitor cells in the fibrous layer. In the knee joint, on the other hand, we did not detect noticeable Ki-67-positive cells in both genotypes, indicating very limited chondrocyte proliferation at 1 month of age.

The growth of TMJ condylar cartilage is regulated by its physiologic loading [36]. In this process, the canonical Wnt/β-catenin signaling is one key mechanosensitive pathway regulating TMJ development [37-39]. We thus tested whether loss of collagen V also alters β-catenin expression (Fig. 9c,d). Consistent with the literature [40], in control mice, β-catenin was found to be actively expressed in the fibrous layer proliferative zone, but not in the hyaline layer. Similar to the Ki-67 expression pattern, in *Col5a1*^{iKO} mice, β-catenin was significantly reduced in the fibrous layer, and absent in the hyaline layer. Also, we did not detect appreciable β-catenin expression in knee cartilage for both genotypes. Therefore, our results indicate that Wnt/β-catenin pathway could be associated with the progenitor cell proliferation and matrix development during condylar cartilage post-natal growth. In turn, collagen V could regulate the proliferation through mediating Wnt/β-catenin signaling. In addition, β-catenin was found in both nucleus and cytoplasm (Fig. 9e), indicating that it may be involved in mechanisms other than canonical Wnt signaling, which involves nuclear translocation of β-catenin [41].

Discussion

Role of collagen V in the post-natal growth of condylar cartilage hyaline layer

This study highlights a distinctive role of collagen V in the establishment of TMJ condylar cartilage ECM, a fibrous-hyaline hybrid (Fig. 10). In condylar cartilage, we found that collagen V impacts the structure and biomechanics of not only the collagen I-dominated fibrous layer, but also the collagen II-rich secondary hyaline layer. In the fibrous layer, the relative high

concentration of collagen V (Fig. 1a), as well as the phenotype observed in *Col5a1*$^{+/-}$ and *Col5a1*^{iKO} mice, support the established structural role of collagen V in regulating collagen I fibril assembly [15]. In the hyaline layer, despite a much lesser presence of collagen V (Fig. 1a), we still detected salient structural and biomechanical defects. In addition, given that the initial steps of collagen fibrillogenesis take place in the PCM [22], the reduction of PCM modulus (Fig. 4d) suggests that collagen V also impacts the early collagen fibril assembly of the hyaline layer. This observation cannot be directly explained by current knowledge of hyaline cartilage ECM, in which, the initial assembly of collagen II fibrils is primarily regulated by collagen XI, not collagen V [42]. In hyaline cartilage, collagen V is only known to play a minor role in adulthood, when one α2(XI) chain is gradually replaced by α1(V) [43]. Indeed, the lack of overt phenotype in *Col5a1*$^{+/-}$ and *Col5a1*^{iKO} knee cartilage (Figs. 6-8) supports limited participation of collagen V in the growth and biomechanical function therein. These observations together point to a unique role of collagen V in regulating the growth of TMJ condylar cartilage. This finding is distinct from current understanding of hyaline cartilage assembly [42] and the established structural role of collagen V [44].

The impact of collagen V on the hyaline layer can be attributed to its regulation of the progenitor cells in the fibrous layer. The condylar cartilage is defined as a "secondary cartilage", which contains a population of *Sox9*-expressing progenitor cells in the fibrous layer (mainly the polymorphic zone) [45]. During post-natal growth, these progenitors maintain their proliferative capability and undergo chondrogenesis, giving rise to the hyaline layer [46, 47]. In contrast, knee articular cartilage does not contain this progenitor population and has limited proliferative capability in post-natal stages [48]. In control mice, a substantial portion of Ki-67-expressing proliferative cells is present in the fibrous layer, but absent in the hyaline layer of condylar

cartilage or knee cartilage (Fig. 9a). The importance of collagen V in mediating progenitor proliferation is highlighted by the reduced Ki-67 activity (Fig. 9a) and cell density in *Col5a1*^{iKO} condyle (Fig. 5e). Thus, collagen V could be a crucial constituent that maintains the progenitor cell microniche. This is in alignment with its higher concentration in the fibrous layer pericellular domain (Fig. 1a), the impairment of PCM with collagen V reduction (Fig. 4d), as well as its role in retaining the muscle stem cell niche [49]. Given that the hyaline layer is established by these progenitors undergoing chondrogenesis during post-natal growth [46, 47], collagen V could regulate the establishment of hyaline layer by mediating the progenitor cell fate and proliferation (Fig. 10).

Mechanobiological regulation of condylar cartilage growth by collagen V

The growth of condylar cartilage is an adaptive process regulated by physiologic TMJ loading [36], during which, the chondrogenesis of progenitor cells and synthesis of sGAGs are suppressed by decreased occlusal loading [50, 51], and enhanced by increased loading [52, 53]. By directly regulating the structure and mechanics of the fibrous layer, collagen V could influence the load transmission to the residing cells of both layers. This is supported by the impairment of the immediate cell microenvironment, i.e., the PCM, in *Col5a1*$^{+/-}$ condylar cartilage (Fig. 4d). In addition, the more pronounced cartilage thinning observed in 2-month-old, but not 1-month-old, *Col5a1*^{iKO} mice (Fig. 5c,d) is contrary to current understanding of collagen V activities. Given that collagen V mainly regulates the initial stage of collagen I fibrillogenesis, it is expected to have a more crucial role in embryonic and neo-natal development than in later stages of post-natal growth [15]. On the other hand, murine TMJ starts to experience extensive physiologic occlusal loading after weaning at 3 weeks of age [32-34]. The more pronounced cartilage thinning observed in the post-weaning 2-month group thus supports an interplay

between collagen V and TMJ loading in condylar cartilage growth. This role is further supported by the observation that the thinning is most pronounced in the central region (Fig. 5d), where the compressive stress is the highest [54], and the hyaline layer is the thickest (Figs. 2b, 5d).

One axis by which collagen V regulates condylar cartilage mechanobiology is through the canonical Wnt/β-catenin pathway. Wnt/β-catenin signaling is a crucial regulator of the craniofacial skeletal development [55], whereby an intricately balanced β-catenin level is required for normal TMJ growth and maintenance. In murine models with both the loss-of-function [37] and gain-of-function [38, 39] of β-catenin, condylar cartilage develops reduced cell proliferation, impaired hyaline cartilage formation, and OA-like degeneration. Here, localization of β-catenin in the fibrous layer and low expression in the pre-hypertrophic and hypertrophic chondrocytes of the hyaline layer (Fig. 9c and [40]) support active involvement of Wnt/β-catenin signaling in the proliferation and chondrogenic differentiation of progenitors. Thus, the reduced β-catenin content in *Col5a1*^{iKO} fibrous layer supports that one mechanism of collagen V mediating the progenitors is through the Wnt/β-catenin pathway. Since Wnt/β-catenin signaling is highly sensitive to mechanical stimuli [56], the impact of collagen V on progenitor proliferation and Wnt/β-catenin signaling can have cross-talk with its regulation of matrix integrity as well as physiologic occlusal loading. In addition, while canonical Wnt signaling induces β-catenin nuclear translocation [41], cytoplasmic β-catenin participates in E-cadherin-catenin-actin complex-mediated cell-cell adhesion and mechanotransduction [57]. In *Col5a1*^{iKO} progenitors, the decreased cytoplasmic β-catenin content (Fig. 9c,e) could also contribute to altered cell-cell adhesion, and thus, the aberrant cell clustering with the loss of collagen V (Figs. 2a,d and 5c,f).

Comparison to the activities of collagen V in knee cartilage

Our results also underscore the stark contrasts of collagen V activities in TMJ condylar cartilage versus knee cartilage. Knee cartilage ECM is dominated by collagen II/IX/XI fibril network entrapping aggrecan-hyaluronan aggregates, and lacks the collagen I-rich fibrous layer [58]. As a primary cartilage tissue, it does not contain the proliferative progenitor population, as supported by the absence of Ki-67 and β-catenin staining (Fig. 9). Thus, the hypothesized activities of collagen V in condylar cartilage (Fig. 10) are not expected to impact knee cartilage, consistent with the lack of structural or biomechanical defects in both *Col5a1*$^{+/-}$ and *Col5a1*^{iKO} mice (Figs. 6-8). Although accelerated cartilage degradation and early OA onset was reported in tendon-specific collagen V knockout mice, such phenotype is expected to be induced by abnormal joint gait and increased laxity due to the impaired tendon and ligament [59]. On the other hand, collagen V is present in the top superficial zone of knee cartilage, albeit at a lower concentration (Fig. 6a), and reduction of collagen V appears to increase the surface fibril heterogeneity (Fig. 7a-c). Since the embryonic development of knee cartilage involves the a population of *Gdf5*-expressing proliferative progenitors [48], collagen V may play a role in this early development process, and collagen V detected on cartilage surface may represent the residual molecules retained from the primitive embryonic matrix. The superficial zone cells have been shown to retain some degree of the stemness or progenitor capacity [60, 61], it is possible that collagen V could have a role in mediating the progenitor cell fate therein, similar to its activities in the TMJ. Thus, despite the lack of overt tissue phenotype, collagen V may have an impact on the early development of knee cartilage or the maintenance of surface progenitors. Further investigations are needed to test these hypothesized activities. To this end, contrast between defects of the two cartilage types observed here supports the tissue- and cell-specific

role of collagen V in mediating progenitor cell fate and mechanically regulated growth of TMJ condylar cartilage (Fig. 10).

Limitations and outlook

This study has several limitations. First, given the wide interactome of collagen V, we have not fully uncovered the mechanisms by which collagen V regulates condylar cartilage growth. For instance, in endothelial cells, collagen V influences fibroblast growth factor-2 (FGF-2)-mediated angiogenesis through binding to FGF-2 via its heparin-binding site and inhibiting FGF-2 signaling [62]. Collagen V was also found to mediate the quiescence of muscle stem cells through the reciprocal Notch-collagen V-calcitonin signaling loop, albeit such role is mainly manifested through its minor α3(V) isoform [49]. In addition, collagen V regulates cell mechanotransduction through mediating the activation of integrins $\alpha_v\beta_3$ and $\alpha_v\beta_5$ in cardiac scar tissues [63], as well as integrins $\alpha_2\beta_1$ and $\alpha_v\beta_3$ in dermal fibroblasts [64]. In the TMJ, collagen V could have also multifaceted roles, and our ongoing studies aim to assess the impact of collagen V on the transcriptome of the condylar cartilage progenitor cells, and thus, to elucidate if collagen V impacts other biological and mechanobiological pathways. Second, we did not focus on collagen XI, which has high structural homology to collagen V [65] and regulates the initial assembly of collagen II fibrils [42]. Given the hybrid nature of condylar cartilage, collagen XI could also have an important regulatory role, especially in the hyaline layer [66, 67]. Recent studies have shown that collagen V and XI can have synergistic activities in regulating tendon fibril structure [68]. Our long-term goal is thus to delineate the individual and coordinated activities of collagens V and XI in the growth and remodeling of condylar cartilage, which will establish a more comprehensive picture of the molecular driving forces that govern the function and disease-associated degeneration of this unique fibrous-hyaline hybrid matrix.

Our results suggest collagen V as a potential target for improving TMJ regeneration. Stem cell-based cartilage regeneration is a promising approach to promote endogenous tissue regeneration without requiring cell transplantation [69, 70]. According to this study, collagen V is a key player in mediating the mechanically regulated growth of condylar cartilage, as it impacts both the matrix assembly and progenitor cell proliferation (Fig. 10). Thus, collagen V can be used in synergy with mechanical stimuli to modulate progenitor cell activities and control synchronized regeneration of the fibrous and hyaline layers. In addition, our results on *Col5a1*$^{+/-}$ mice provide the basis for understanding the higher propensity of TMD in cEDS patients [71], and may assist the development of improved patient care. On the technical front, this study is the first to quantify the structural and biomechanical phenotype of condylar cartilage in genetic murine models. Our results demonstrate that integrating advanced AFM-nanomechanical tools with imaging assays will enable a thorough evaluation of the integrity and function-relevant biomechanical properties of TMJ in various genetic or disease murine models.

Conclusions

In summary, this study is the first to query the matrix molecular activities that give rise to the fibrous-hyaline hybrid ECM of TMJ condylar cartilage. Results highlight a crucial role of collagen V in this process. In addition to its expected role in regulating the fibrillar structure of fibrous layer, collagen V also regulates the formation of hyaline layer. The impact of collagen V on the hyaline layer can be attributed to its role in regulating the proliferation of progenitor cells in the fibrous layer (Fig. 10). Such impact is coupled with the mechanically regulated TMJ growth, and is mediated through the canonical Wnt/β-catenin pathway. This role of collagen V in retaining the progenitor cell niche is specific to the secondary cartilage nature of TMJ condyle, as loss of collagen V does not impact the post-natal growth of knee cartilage, a primary cartilage

without the highly proliferative progenitor cells. These findings will advance the understanding of collagen V activities in multiple tissue types, and provide a new foundation for future studies to improve condylar cartilage regeneration by designing collagen V-targeting gene therapy [72] or collagen V-derived peptides and biomaterials [73].

Methods

Animal model

Col5a1$^{+/-}$ [15] and *Col5a1*^{iKO} (*Col5a1*$^{flox/flox}$/*Rosa26Cre*^{ER}) [18] mice in the C57BL/6 strain were generated as previously described and were housed in the Calhoun animal facility at Drexel University. To induce the knockout of *Col5a1* gene, tamoxifen (T5648, Sigma) was intraperitoneally (i.p.) injected into *Col5a1*^{iKO} mice at 4.5 mg per 40 g of body weight per day for 3 consecutive days in the form of 20 mg/mL suspended in sesame oil (S3547, Sigma) with 1% benzyl alcohol (305197, Sigma). By day 5, the excision of *Col5a1* expression in TMJ condylar cartilage was confirmed by qPCR (forward primer: 5'-AAGCGTGGGAAACTGCTCTCCTAT-3', reverse primer: 5'-AGCAGTTGTAGGTGACGTTCTGGT-3'). The knockout was induced at 1 week and 1 month of ages, and mice were sacrificed at 1 and 2 months of ages, respectively. For *Col5a1*$^{+/-}$ mice, age-matched WT littermates from the breeding of *Col5a1*$^{+/-}$ mice were used as controls. For *Col5a1*^{iKO} mice, two control groups were used, including *Col5a1*$^{flox/flox}$/*Rosa26Cre*^{ER} mice injected with vehicle (the same amount of sesame oil and benzyl alcohol but without tamoxifen) and WT mice injected with tamoxifen at the same dosage and frequency. We found no differences between these two groups. We also found no significant differences between male and female mice, and thus, both genders were included in this study.

All animal studies were approved by the Institutional Animal Care and Use Committee at Drexel University.

Histology and immunofluorescence imaging

TMJs and knee joints were harvested, fixed in 4% paraformaldehyde in PBS (Santa Cruz Biotech) for 24 hrs, decalcified in 10% ethylene-diaminetetraacetic acid (EDTA, pH ≈ 7.4, E9884, Sigma) over 14-21 days. Serial 6-μm-thick sagittal sections were prepared, and one out of every five sections were stained with Safranin-O/Fast Green or Hematoxylin/Eosin (H&E), and imaged with a Zeiss Axio Observer microscope (Carl Zeiss). For TMJ, a 200 × 100 μm^2 region of interest (ROI) was defined to include anterior, central and posterior domains. In each ROI, the thickness and cell density were measured separately for the fibrous and uncalcified hyaline layers, as directed by the staining for sGAGs and cell morphology using ImageJ [74]. Similar procedure was applied to quantify cartilage thickness and cell density in knee joint ($n \geq 5$). For both joints, we assessed cell arrangement scores on H&E-stained sections based on the established semi-quantitative metrics [75].

Immunofluorescence (IF) imaging was performed on additional sections ($n \geq 4$ to confirm repeatability). Sections were first incubated with Bloxall (SP-6000, Vector Labs) to quench endogenous peroxidases and phosphatases activities, and then, stained with primary antibodies overnight at 4°C (collagen V: AB7046, Abcam, 1:100 dilution; collagen I: AB34710, 1:100; collagen II: AB34712, 1:100; aggrecan: AB1031, MilliporeSigma, 1:100; collagen VI: 70R-CR009X, Fitzgerald, MA, 1:200; perlecan: A7L6, ThermoFisher, 1:200; Ki-67: 550609, BD Biosciences, 1:50, β-catenin: 610153, BD Biosciences, 1:50). For matrix molecules, sections were then incubated with the secondary antibody (AlexaFlour 488nm, A-11037, ThermoFisher,

1:250) at room temperature for 1 hr. For Ki-67 and β-catenin, sections were incubated with HRP horse anti-mouse IgG (MP-7402, Vector Labs) for 1 hr, and then, stained with TSA fluorescein reagent (SAT701001EA, Akoya Biosciences) for 8 min. Immunofluorescence images were taken with a DM6000B fluorescence microscope (Leica) or a DMi8 confocal microscope (Leica). For all images, sections incubated without the primary antibody but with the secondary antibody were included as internal negative controls to confirm the specificity. For Ki-67 and β-catenin images taken on TMJ condylar cartilage, we analyzed the percentage of Ki-67 positive cells, and relative β-catenin intensity normalized by the DAPI number within the fibrous layer in each 150 × 50 μm^2 ROI using ImageJ (n = 5/genotype).

Collagen nanostructural analysis.

Scanning electron microscopy (SEM) was applied to quantify collagen fibril structure on the surfaces of condylar cartilage and knee cartilage, following the established procedure [76]. Immediately after AFM-nanoindentation, joints were processed for proteoglycan removal, fixed and dehydrated, air dried overnight, coated with ≈ 6 nm thick platinum-palladium mixture, and then, imaged using a Supra 50 VP SEM (Carl Zeiss). Transmission electron microscopy (TEM) was applied to delineate the collagen fibril structure in the interior fibrous and hyaline layers of condylar cartilage ECM, following the established procedure [77]**.** Additional freshly dissected condyles were fixed, dehydrated, processed, embedded for the preparation of ~ 90 nm cross-sections, and then, imaged using a JOEL 1400 TEM (JOEL). We then quantified collagen fibril diameters for each region using ImageJ (FIJI).

AFM-based nanomechanical analysis

AFM-nanoindentation was performed on the surfaces of freshly dissected TMJ condylar cartilage and femoral condyle knee cartilage using custom-made microspherical colloidal tips ($R \approx 5$ μm, nominal $k \approx 2$ N/m, NSC36-B for TMJ; $R \approx 5$ μm, $k \approx 5.4$ N/m, NSC35-C for knee cartilage, NanoAndMore) and a Dimension Icon AFM (Bruker Nano) at ≈ 10 μm/s rate in 1× PBS with protease inhibitors (Pierce 88266, ThermoFisher), following our established procedure [78]. For each sample, at least 10-15 locations were tested to account for spatial heterogeneity. The indentation modulus, E_{ind}, was calculated by fitting the entire loading portion of the *F-D* curve with Hertz model, assuming Poisson's ratio $v \approx 0$ for condylar cartilage [79], and 0.1 for knee cartilage [80].

For the quantification of the hyaline layer mechanical properties, freshly dissected TMJ condyles were embedded in optimum cutting temperature (OCT) medium to prepare ≈ 6-μm-thick, unfixed sagittal sections via Kawamoto's film-assisted cryo-sectioning [81]. Following the established procedure, sections were immunolabelled with perlecan (primary antibody: A7L6, ThermoFisher, 1:50 for 20 min, secondary antibody: goat anti-rat IgG, 28903, Rockland, 1:200, for 20 min at room temperature), and immediately tested by AFM [82]. Guided by perlecan IF-imaging, AFM-nanomechanical mapping was performed using microspherical tips ($R \approx 2.25$ μm, $k \approx 1$ N/m, NSC36-A, NanoAndMore) and MFP-3D AFM (Asylum Research) in 1× PBS with protease inhibitors. For each map, we acquired *F-D* curves from 30 × 30 indentation grid within a 15 × 15 μm^2 ROI (or a 40 × 40 grid within a 20 × 20 μm^2 ROI), consisting of ring shaped PCM domains and the further-removed, territorial/interterritorial extracellular matrix (T/IT-ECM) [30, 76]. The modulus, E_{ind}, was calculated via the finite thickness corrected Hertz model [29], assuming $v \approx 0.05$ for the hyaline layer [23].

Statistical analysis

To avoid the assumption of normal distribution of the data, nonparametric statistical tests were applied to test the significance between genotypes. Mann-Whitney U test was applied to compare cartilage thickness, cell density, cell arrangement scores, relative IF intensity, gene expression and E_{ind}, using the average values of each animal. For collagen nanostructural data, since ≥ 350 fibrils were measured for each region and each genotype, based on the central limit theorem, unpaired two-sample *t*-test was applied to compare the mean fibril diameters, and two-sample *F*-test was applied to compare the fibril diameter variances. For outcomes involving multiple comparisons across tissue regions, such as cartilage thickness and collagen fibril diameter, E_{ind} of PCM and T/IT-ECM, Holm-Bonferroni correction was applied to adjust for family-wise type I errors [83]. In all the tests, the significance level was set at $\alpha = 0.05$.

Author Contributions

Conceptualization: L.H.; Supervision: L.H.; Data Collection and Analysis: P.C., B.K., B.H., S.M.A., C.W., D.R.C.; Data Interpretation: P.C., B.K., B.H., R.L.M., N.A.D., X.L.L., D.B.F., E.K., D.E.B., L.H.; Writing: P.C., B.K., B.H., X.L.L., E.K., L.H.; Funding Acquisition: L.H. All authors intellectually contributed and provided approval for publication.

Acknowledgements

This work was financially supported by the National Science Foundation (NSF) Grant CMMI-1751898 (to LH), National Institutes of Health (NIH) Grant R21DE029567 (to LH), as well as NIH Grant P30AR069619 to the Penn Center for Musculoskeletal Disorders. We thank the Singh Center for Nanotechnology at the University of Pennsylvania for the use of TIRF MFP-3D, which is part of the National Nanotechnology Coordinated Infrastructure Program supported by the NSF Grant NNCI-1542153. We thank Dr. L. J. Soslowsky (University of

Pennsylvania) for the kind help with murine TMJ samples, and Dr. M. Enomoto-Iwamoto (University of Maryland, Baltimore) for insightful discussions.

Abbreviations Used

AFM, atomic force microscopy; cEDS, classic Ehlers-Danlos syndrome; ECM, extracellular matrix; FGF, fibroblast growth factor; IF, immunofluorescence; MFP, molecular force probe; OCT, optimum cutting temperature; PBS, phosphate buffered saline; PCM, pericellular matrix; qPCR, quantitative polymerase chain reaction; ROI, region of interest; SEM, scanning electron microscopy; sGAG, sulfated glycosaminoglycan; T/IT-ECM, territorial/interterritorial extracellular matrix; TEM, transmission electron microscopy; TIRF, total internal reflection fluorescence; TM, tamoxifen; TMD, temporomandibular joint disorder; TMJ, temporomandibular joint; WT, wild-type.

References

[1] Prevalence of TMJD and its Signs and Symptoms. 2018. National Institute of Dental and Craniofacial Research. https://www.nidcr.nih.gov/research/data-statistics/facial-pain/prevalence.

[2] S. Kuroda, K. Tanimoto, T. Izawa, S. Fujihara, J.H. Koolstra, E. Tanaka, Biomechanical and biochemical characteristics of the mandibular condylar cartilage, Osteoarthritis Cartilage 17 (11) (2009) 1408-1415.

[3] A.R. Chin, J. Gao, Y. Wang, J.M. Taboas, A.J. Almarza, Regenerative potential of various soft polymeric scaffolds in the temporomandibular joint condyle, J. Oral Maxillofac. Surg. 76 (9) (2018) 2019-2026.

[4] X.D. Wang, J.N. Zhang, Y.H. Gan, Y.H. Zhou, Current understanding of pathogenesis and treatment of TMJ osteoarthritis, J. Dent. Res. 94 (5) (2015) 666-673.

[5] E. Tanaka, J.H. Koolstra, Biomechanics of the temporomandibular joint, J. Dent. Res. 87 (11) (2008) 989-991.

[6] M. Singh, M.S. Detamore, Tensile properties of the mandibular condylar cartilage, J. Biomech. Eng. 130 (1) (2008) 011009.

[7] J. Chen, A. Utreja, Z. Kalajzic, T. Sobue, D. Rowe, S. Wadhwa, Isolation and characterization of murine mandibular condylar cartilage cell populations, Cells Tissues Organs 195 (3) (2012) 232-243.

[8] A. Maroudas, Physicochemical properties of articular cartilage, in: M.A.R. Freeman (Ed.), Adult Articular Cartilage, Pitman, England, 1979, pp. 215-290.

[9] M. Urbanczyk, S.L. Layland, K. Schenke-Layland, The role of extracellular matrix in biomechanics and its impact on bioengineering of cells and 3D tissues, Matrix Biol. 85-86 (2020) 1-14.

[10] R.V. Iozzo, M.A. Gubbiotti, Extracellular matrix: the driving force of mammalian diseases, Matrix Biol. 71-72 (2018) 1-9.

[11] N.K. Karamanos, A.D. Theocharis, T. Neill, R.V. Iozzo, Matrix modeling and remodeling: a biological interplay regulating tissue homeostasis and diseases, Matrix Biol. 75-76 (2019) 1-11.

[12] K.Y. DeLeon-Pennell, T.H. Barker, M.L. Lindsey, Fibroblasts: the arbiters of extracellular matrix remodeling, Matrix Biol. 91-92 (2020) 1-7.

[13] S. Ricard-Blum, S.D. Vallet, Fragments generated upon extracellular matrix remodeling: biological regulators and potential drugs, Matrix Biol. 75-76 (2019) 170-189.

[14] E. Shimshoni, I. Adir, R. Afik, I. Solomonov, A. Shenoy, M. Adler, L. Puricelli, F. Sabino, S. Savickas, O. Mouhadeb, N. Gluck, S. Fishman, L. Werner, T.M. Salame, D.S. Shouval, C. Varol, U. Auf dem Keller, A. Podestà, T. Geiger, P. Milani, U. Alon, I. Sagi, Distinct extracellular-matrix remodeling events precede symptoms of inflammation, Matrix Biol. 96 (2021) 47-68.

[15] R.J. Wenstrup, J.B. Florer, E.W. Brunskill, S.M. Bell, I. Chervoneva, D.E. Birk, Type V collagen controls the initiation of collagen fibril assembly, J. Biol. Chem. 279 (51) (2004) 53331-53337.

[16] T.F. Linsenmayer, E. Gibney, F. Igoe, M.K. Gordon, J.M. Fitch, L.I. Fessler, D.E. Birk, Type V collagen: molecular structure and fibrillar organization of the chicken alpha 1(V) NH_2-terminal domain, a putative regulator of corneal fibrillogenesis, J. Cell Biol. 121 (5) (1993) 1181-1189.

[17] B.K. Connizzo, L. Han, D.E. Birk, L.J. Soslowsky, Collagen V-heterozygous and -null supraspinatus tendons exhibit altered dynamic mechanical behaviour at multiple hierarchical scales, Interface Focus 6 (1) (2016) 20150043.
[18] M. Sun, S. Chen, S.M. Adams, J.B. Florer, H. Liu, W.W. Kao, R.J. Wenstrup, D.E. Birk, Collagen V is a dominant regulator of collagen fibrillogenesis: dysfunctional regulation of structure and function in a corneal-stroma-specific Col5a1-null mouse model, J. Cell Sci. 124 (23) (2011) 4096-4105.
[19] R.J. Wenstrup, J.B. Florer, W.G. Cole, M.C. Willing, D.E. Birk, Reduced type I collagen utilization: a pathogenic mechanism in COL5A1 haplo-insufficient Ehlers-Danlos syndrome, J. Cell. Biochem. 92 (1) (2004) 113-124.
[20] L.A. Norton, L.A. Assael, Orthodontic and temporomandibular joint considerations in treatment of patients with Ehlers-Danlos syndrome, Am. J. Orthod. Dentofacial Orthop. 111 (1) (1997) 75-84.
[21] F. Malfait, R.J. Wenstrup, A. De Paepe, Clinical and genetic aspects of Ehlers-Danlos syndrome, classic type, Genet. Med. 12 (10) (2010) 597-605.
[22] S.M. Smith, G. Zhang, D.E. Birk, Collagen V localizes to pericellular sites during tendon collagen fibrillogenesis, Matrix Biol. 33 (2014) 47-53.
[23] L. Ruggiero, B.K. Zimmerman, M. Park, L. Han, L. Wang, D.L. Burris, X.L. Lu, Roles of the fibrous superficial zone in the mechanical behavior of TMJ condylar cartilage, Ann. Biomed. Eng. 43 (2015) 2652-2662.
[24] F. Guilak, R.J. Nims, A. Dicks, C.L. Wu, I. Meulenbelt, Osteoarthritis as a disease of the cartilage pericellular matrix, Matrix Biol. 71-72 (2018) 40-50.
[25] J. Sanchez-Adams, R.E. Wilusz, F. Guilak, Atomic force microscopy reveals regional variations in the micromechanical properties of the pericellular and extracellular matrices of the meniscus, J. Orthop. Res. 31 (8) (2013) 1218-1225.
[26] E.J. Vanderploeg, C.G. Wilson, S.M. Imler, C.H. Ling, M.E. Levenston, Regional variations in the distribution and colocalization of extracellular matrix proteins in the juvenile bovine meniscus, J. Anat. 221 (2) (2012) 174-186.
[27] Q. Li, B. Han, C. Wang, W. Tong, W.J. Tseng, L.-H. Han, X.S. Liu, M. Enomoto-Iwamoto, R.L. Mauck, L. Qin, R.V. Iozzo, D.E. Birk, L. Han, Mediation of cartilage matrix degeneration and fibrillation by decorin in post-traumatic osteoarthritis, Arthritis Rheumatol. 72 (8) (2020) 1266-1277.
[28] B. Han, Q. Li, C. Wang, P. Chandrasekaran, Y. Zhou, L. Qin, X.S. Liu, M. Enomoto-Iwamoto, D. Kong, R.V. Iozzo, D.E. Birk, L. Han, Differentiated activities of decorin and biglycan in the progression of post-traumatic osteoarthritis, Osteoarthritis Cartilage (2021) In press, doi: 10.1016/j.joca.2021.1003.1019.
[29] E.K. Dimitriadis, F. Horkay, J. Maresca, B. Kachar, R.S. Chadwick, Determination of elastic moduli of thin layers of soft material using the atomic force microscope, Biophys. J. 82 (5) (2002) 2798-2810.
[30] D.R. Chery, B. Han, Q. Li, Y. Zhou, S.J. Heo, B. Kwok, P. Chandrasekaran, C. Wang, L. Qin, X.L. Lu, D. Kong, M. Enomoto-Iwamoto, R.L. Mauck, L. Han, Early changes in cartilage pericellular matrix micromechanobiology portend the onset of post-traumatic osteoarthritis, Acta Biomater. 111 (2020) 267-278.
[31] D.R. Chery, B. Han, Y. Zhou, C. Wang, S.M. Adams, P. Chandrasekaran, B. Kwok, S.-J. Heo, M. Enomoto-Iwamoto, X.L. Lu, D. Kong, R.V. Iozzo, D.E. Birk, R.L. Mauck, L. Han,

Decorin regulates cartilage pericellular matrix micromechanobiology, Matrix Biol. 96 (2021) 1-17.
[32] G. Shen, M.A. Darendeliler, The adaptive remodeling of condylar cartilage - a transition from chondrogenesis to osteogenesis, J. Dent. Res. 84 (8) (2005) 691-699.
[33] A. Utreja, N.A. Dyment, S. Yadav, M.M. Villa, Y. Li, X. Jiang, R. Nanda, D.W. Rowe, Cell and matrix response of temporomandibular cartilage to mechanical loading, Osteoarthritis Cartilage 24 (2) (2016) 335-344.
[34] R. Kaul, M.H. O'Brien, E. Dutra, A. Lima, A. Utreja, S. Yadav, The effect of altered loading on mandibular condylar cartilage, PLoS One 11 (7) (2016) e0160121.
[35] T. Scholzen, J. Gerdes, The Ki-67 protein: from the known and the unknown, J. Cell. Physiol. 182 (3) (2000) 311-322.
[36] B.F. Betti, V. Everts, J.C.F. Ket, H. Tabeian, A.D. Bakker, G.E. Langenbach, F. Lobbezoo, Effect of mechanical loading on the metabolic activity of cells in the temporomandibular joint: a systematic review, Clin. Oral Investig. 22 (1) (2018) 57-67.
[37] Y. Jing, J. Jing, K. Wang, K. Chan, S.E. Harris, R.J. Hinton, J.Q. Feng, Vital roles of β-catenin in trans-differentiation of chondrocytes to bone cells, Int. J. Biol. Sci. 14 (1) (2018) 1-9.
[38] M. Wang, S. Li, W. Xie, J. Shen, H.J. Im, J.D. Holz, M. Wang, T.G. Diekwisch, D. Chen, Activation of β-catenin signalling leads to temporomandibular joint defects, Eur. Cell Mater. 28 (2014) 223-235.
[39] T. Hui, Y. Zhou, T. Wang, J. Li, S. Zhang, L. Liao, J. Gu, L. Ye, L. Zhao, D. Chen, Activation of β-catenin signaling in aggrecan-expressing cells in temporomandibular joint causes osteoarthritis-like defects, Int. J. Oral Sci. 10 (2) (2018) 13.
[40] K. Chen, H. Quan, G. Chen, D. Xiao, Spatio-temporal expression patterns of Wnt signaling pathway during the development of temporomandibular condylar cartilage, Gene Expr. Patterns 25-26 (2017) 149-158.
[41] B.T. MacDonald, K. Tamai, X. He, Wnt/β-catenin signaling: components, mechanisms, and diseases, Dev. Cell 17 (1) (2009) 9-26.
[42] D.R. Eyre, M.A. Weis, J.-J. Wu, Articular cartilage collagen: an irreplaceable framework?, Eur. Cell Mater. 12 (2006) 57-63.
[43] J.J. Wu, M.A. Weis, L.S. Kim, B.G. Carter, D.R. Eyre, Differences in chain usage and cross-linking specificities of cartilage type V/XI collagen isoforms with age and tissue, J. Biol. Chem. 284 (9) (2009) 5539-5545.
[44] D.E. Birk, P. Brückner, Collagens, suprastructures, and collagen fibril assembly, in: R.P. Mecham (Ed.), The Extracellular Matrix: an Overview, Springer-Verlag, Berlin, 2011, pp. 77-115.
[45] M. Delatte, J.W. Von den Hoff, R.E. van Rheden, A.M. Kuijpers-Jagtman, Primary and secondary cartilages of the neonatal rat: the femoral head and the mandibular condyle, Eur. J. Oral Sci. 112 (2) (2004) 156-162.
[46] M.C. Embree, M. Chen, S. Pylawka, D. Kong, G.M. Iwaoka, I. Kalajzic, H. Yao, C. Shi, D. Sun, T.J. Sheu, D.A. Koslovsky, A. Koch, J.J. Mao, Exploiting endogenous fibrocartilage stem cells to regenerate cartilage and repair joint injury, Nat. Commun. 7 (2016) 13073.
[47] N. Kurio, C. Saunders, T.E. Bechtold, I. Salhab, H.D. Nah, S. Sinha, P.C. Billings, M. Pacifici, E. Koyama, Roles of Ihh signaling in chondroprogenitor function in postnatal condylar cartilage, Matrix Biol. 67 (2018) 15-31.

[48] R.S. Decker, H.B. Um, N.A. Dyment, N. Cottingham, Y. Usami, M. Enomoto-Iwamoto, M.S. Kronenberg, P. Maye, D.W. Rowe, E. Koyama, M. Pacifici, Cell origin, volume and arrangement are drivers of articular cartilage formation, morphogenesis and response to injury in mouse limbs, Dev. Biol. 426 (1) (2017) 56-68.
[49] M.B. Baghdadi, D. Castel, L. Machado, S.I. Fukada, D.E. Birk, F. Relaix, S. Tajbakhsh, P. Mourikis, Reciprocal signalling by Notch-Collagen V-CALCR retains muscle stem cells in their niche, Nature 557 (7707) (2018) 714-718.
[50] J. Chen, K.P. Sorensen, T. Gupta, T. Kilts, M. Young, S. Wadhwa, Altered functional loading causes differential effects in the subchondral bone and condylar cartilage in the temporomandibular joint from young mice, Osteoarthritis Cartilage 17 (3) (2009) 354-361.
[51] E.H. Dutra, O.B. MH, A. Lima, Z. Kalajzic, A. Tadinada, R. Nanda, S. Yadav, Cellular and matrix response of the mandibular condylar cartilage to botulinum toxin, PLoS One 11 (10) (2016) e0164599.
[52] T. Sobue, W.C. Yeh, A. Chhibber, A. Utreja, V. Diaz-Doran, D. Adams, Z. Kalajzic, J. Chen, S. Wadhwa, Murine TMJ loading causes increased proliferation and chondrocyte maturation, J. Dent. Res. 90 (4) (2011) 512-516.
[53] Q. Liu, H.X. Yang, J. Duan, H.Y. Zhang, M.J. Xie, H.T. Ren, M. Zhang, J. Zhang, L. Lu, X.D. Liu, S.B. Yu, M.Q. Wang, Bilateral anterior elevation prosthesis boosts chondrocytes proliferation in mice mandibular condyle, Oral Dis. 25 (6) (2019) 1589-1599.
[54] V. Colombo, S. Palla, L.M. Gallo, Temporomandibular joint loading patterns related to joint morphology: a theoretical study, Cells Tissues Organs 187 (4) (2008) 295-306.
[55] M. Nagayama, M. Iwamoto, A. Hargett, N. Kamiya, Y. Tamamura, B. Young, T. Morrison, H. Takeuchi, M. Pacifici, M. Enomoto-Iwamoto, E. Koyama, Wnt/β-catenin signaling regulates cranial base development and growth, J. Dent. Res. 87 (3) (2008) 244-249.
[56] C.M. Warboys, Mechanoactivation of Wnt/β-catenin pathways in health and disease, Emerg. Top. Life Sci. 2 (5) (2018) 701-712.
[57] S. Yamada, S. Pokutta, F. Drees, W.I. Weis, W.J. Nelson, Deconstructing the cadherin-catenin-actin complex, Cell 123 (5) (2005) 889-901.
[58] L. Han, A.J. Grodzinsky, C. Ortiz, Nanomechanics of the cartilage extracellular matrix, Annu. Rev. Mater. Res. 41 (2011) 133-168.
[59] M. Sun, B.K. Connizzo, S.M. Adams, B.R. Freedman, R.J. Wenstrup, L.J. Soslowsky, D.E. Birk, Targeted deletion of collagen V in tendons and ligaments results in a classic Ehlers-Danlos syndrome joint phenotype, Am. J. Pathol. 185 (5) (2015) 1436-1447.
[60] G.P. Dowthwaite, J.C. Bishop, S.N. Redman, I.M. Khan, P. Rooney, D.J. Evans, L. Haughton, Z. Bayram, S. Boyer, B. Thomson, M.S. Wolfe, C.W. Archer, The surface of articular cartilage contains a progenitor cell population, J. Cell Sci. 117 (6) (2004) 889-897.
[61] S. Hattori, C. Oxford, A.H. Reddi, Identification of superficial zone articular chondrocyte stem/progenitor cells, Biochem. Biophys. Res. Commun. 358 (1) (2007) 99-103.
[62] T. Jia, E. Vaganay, G. Carpentier, P. Coudert, V. Guzman-Gonzales, R. Manuel, B. Eymin, J.L. Coll, F. Ruggiero, A collagen Vα1-derived fragment inhibits FGF-2 induced-angiogenesis by modulating endothelial cells plasticity through its heparin-binding site, Matrix Biol. 94 (2020) 18-30.
[63] T. Yokota, J. McCourt, F. Ma, S. Ren, S. Li, T.H. Kim, Y.Z. Kurmangaliyev, R. Nasiri, S. Ahadian, T. Nguyen, X.H.M. Tan, Y. Zhou, R. Wu, A. Rodriguez, W. Cohn, Y. Wang, J. Whitelegge, S. Ryazantsev, A. Khademhosseini, M.A. Teitell, P.Y. Chiou, D.E. Birk, A.C.

Rowat, R.H. Crosbie, M. Pellegrini, M. Seldin, A.J. Lusis, A. Deb, Type V collagen in scar tissue regulates the size of scar after heart injury, Cell 182 (3) (2020) 545-562.e523.
[64] N. Zoppi, R. Gardella, A. De Paepe, S. Barlati, M. Colombi, Human fibroblasts with mutations in *COL5A1* and *COL3A1* genes do not organize collagens and fibronectin in the extracellular matrix, down-regulate $\alpha_2\beta_1$ integrin, and recruit $\alpha_V\beta_3$ instead of $\alpha_5\beta_1$ integrin, J. Biol. Chem. 279 (18) (2004) 18157-18168.
[65] S.M. Smith, D.E. Birk, Focus on molecules: collagens V and XI, Exp. Eye Res. 98 (1) (2012) 105-106.
[66] L. Xu, C.M. Flahiff, B.A. Waldman, D. Wu, B.R. Olsen, L.A. Setton, Y. Li, Osteoarthritis-like changes and decreased mechanical function of articular cartilage in the joints of mice with the chondrodysplasia gene (*cho*), Arthritis Rheum. 48 (9) (2003) 2509-2518.
[67] N.P. Lam, Y. Li, A.B. Waldman, J. Brussiau, P.L. Lee, B.R. Olsen, L. Xu, Age-dependent increase of discoidin domain receptor 2 and matrix metalloproteinase 13 expression in temporomandibular joint cartilage of type IX and type XI collagen-deficient mice, Arch. Oral Biol. 52 (6) (2007) 579-584.
[68] M. Sun, E.Y. Luo, S.M. Adams, T. Adams, Y. Ye, S.S. Shetye, L.J. Soslowsky, D.E. Birk, Collagen XI regulates the acquisition of collagen fibril structure, organization and functional properties in tendon, Matrix Biol. 94 (2020) 77-94.
[69] H. Nie, C.H. Lee, J. Tan, C. Lu, A. Mendelson, M. Chen, M.C. Embree, K. Kong, B. Shah, S. Wang, S. Cho, J.J. Mao, Musculoskeletal tissue engineering by endogenous stem/progenitor cells, Cell Tissue Res. 347 (3) (2012) 665-676.
[70] C.H. Lee, F.Y. Lee, S. Tarafder, K. Kao, Y. Jun, G. Yang, J.J. Mao, Harnessing endogenous stem/progenitor cells for tendon regeneration, J. Clin. Invest. 125 (7) (2015) 2690-2701.
[71] P.H. Byers, M.L. Murray, Ehlers-Danlos syndrome: a showcase of conditions that lead to understanding matrix biology, Matrix Biol. 33 (2014) 10-15.
[72] C. Bonod-Bidaud, M. Roulet, U. Hansen, A. Elsheikh, M. Malbouyres, S. Ricard-Blum, C. Faye, E. Vaganay, P. Rousselle, F. Ruggiero, In vivo evidence for a bridging role of a collagen V subtype at the epidermis-dermis interface, J. Invest. Dermatol. 132 (7) (2012) 1841-1849.
[73] L.E. de Castro Brás, N.G. Frangogiannis, Extracellular matrix-derived peptides in tissue remodeling and fibrosis, Matrix Biol. 91-92 (2020) 176-187.
[74] B. Han, Q. Li, C. Wang, P. Patel, S.M. Adams, B. Doyran, H.T. Nia, R. Oftadeh, S. Zhou, C.Y. Li, X.S. Liu, X.L. Lu, M. Enomoto-Iwamoto, L. Qin, R.L. Mauck, R.V. Iozzo, D.E. Birk, L. Han, Decorin regulates the aggrecan network integrity and biomechanical functions of cartilage extracellular matrix, ACS Nano 13 (10) (2019) 11320-11333.
[75] L. Xu, I. Polur, C. Lim, J.M. Servais, J. Dobeck, Y. Li, B.R. Olsen, Early-onset osteoarthritis of mouse temporomandibular joint induced by partial discectomy, Osteoarthritis Cartilage 17 (7) (2009) 917-922.
[76] C. Wang, B.K. Brisson, M. Terajima, Q. Li, K. Hoxha, B. Han, A.M. Goldberg, X.S. Liu, M.S. Marcolongo, M. Enomoto-Iwamoto, M. Yamauchi, S.W. Volk, L. Han, Type III collagen is a key regulator of the collagen fibrillar structure and biomechanics of articular cartilage and meniscus, Matrix Biol. 85-86 (2020) 47-67.
[77] H.L. Ansorge, X. Meng, G. Zhang, G. Veit, M. Sun, J.F. Klement, D.P. Beason, L.J. Soslowsky, M. Koch, D.E. Birk, Type XIV collagen regulates fibrillogenesis: premature collagen fibril growth and tissue dysfunction in null mice, J. Biol. Chem. 284 (13) (2009) 8427-8438.

[78] P. Chandrasekaran, B. Doyran, Q. Li, B. Han, T.E. Bechtold, E. Koyama, X.L. Lu, L. Han, Biomechanical properties of murine TMJ articular disc and condyle cartilage via AFM-nanoindentation, J. Biomech. 60 (2017) 134-141.
[79] C.K. Hagandora, T.W. Chase, A.J. Almarza, A comparison of the mechanical properties of the goat temporomandibular joint disc to the mandibular condylar cartilage in unconfined compression, J. Dent. Biomech. 2011 (2011) 212385.
[80] M.D. Buschmann, Y.-J. Kim, M. Wong, E. Frank, E.B. Hunziker, A.J. Grodzinsky, Stimulation of aggrecan synthesis in cartilage explants by cyclic loading is localized to regions of high interstitial fluid flow, Arch. Biochem. Biophys. 366 (1) (1999) 1-7.
[81] T. Kawamoto, K. Kawamoto, Preparation of thin frozen sections from nonfixed and undecalcified hard tissues using Kawamot's film method (2012), Methods Mol. Biol. 1130 (2014) 149-164.
[82] N.A. Zelenski, H.A. Leddy, J. Sanchez-Adams, J. Zhang, P. Bonaldo, W. Liedtke, F. Guilak, Type VI collagen regulates pericellular matrix properties, chondrocyte swelling, and mechanotransduction in mouse articular cartilage, Arthritis Rheumatol. 67 (5) (2015) 1286-1294.
[83] S. Holm, A simple sequentially rejective multiple test procedure, Scand. J. Stat. 6 (2) (1979) 65-70.

Figure Captions

Figure 1 Immunofluorescence (IF) images of matrix molecules in the extracellular matrix (ECM) of wild-type (+/+) and *Col5a1*$^{+/-}$ (+/−) murine TMJ condylar cartilage at 3 months of age, including **a)** collagen V, **b)** collagen I, **c)** collagen II, **d)** aggrecan, **e)** collagen VI and **f)** perlecan (blue: DAPI; F: fibrous layer; H: hyaline layer). The negative control is shown at the bottom ($n \geq 4$).

Figure 2 Impact of collagen V reduction on the gross-level morphology of TMJ condylar cartilage. **a)** Hematoxylin and Eosin (H&E, top panel) and Safranin-O/Fast Green (bottom panel) histology images of wild-type (+/+) and *Col5a1*$^{+/-}$ (+/−) murine TMJ condyle at 3 months of age show no appreciable changes in cartilage morphology or sulfated glycosaminoglycan (sGAG) staining, but altered cell density and arrangement (black arrowheads). **b)** Cartilage thickness, **c)** cellular density and **d)** cell arrangement score measured on each of the fibrous (F) and hyaline (H) layer of TMJ condylar cartilage at 3 months of age ($n \geq 5$, mean ± 95% CI, *: $p < 0.05$). Each data point represents the average value measured from one animal.

Figure 3 Impact of collagen V reduction on the nanostructure of collagen fibrils on the surface and matrix interior of TMJ condylar cartilage. **a)** Representative electron microscopy images of collagen fibril nanostructure of wild-type (+/+) and *Col5a1*$^{+/-}$ (+/−) murine TMJ condyle at 3 months of age: surface via SEM, as well as the fibrous and hyaline layers of the matrix interior via TEM. **b)** Histogram of fibril diameter distribution, d_{col} (> 350 fibrils from $n = 3$ animals for each genotype in each region). Shown together are the normal distribution, $N(\mu, \sigma^2)$, fits to fibril diameters (for each fit, values of μ and σ correspond to the mean and standard deviation of fibril diameters). **c)** Comparison of fibril diameter heterogeneity (variance) between the two genotypes (mean ± 95% CI). For data in panels b and c, adjusted $p < 0.0001$ between WT and *Col5a1*$^{+/-}$ groups for all three regions.

Figure 4 Impact of collagen V reduction on the biomechanical properties of TMJ condylar cartilage. **a)** Representative AFM-nanoindentation force versus depth, *F-D*, curves measured on the central regions of wild-type (+/+) and *Col5a1*$^{+/-}$ (+/−) murine TMJ condyle surfaces at 3 months of age. The symbols are experimental data (density reduced for clarity), and solid lines are associated Hertz model fits to the entire loading portion of each *F-D* curve. **b)** Comparison of the indention modulus, E_{ind}, between the two genotypes (mean ± 95% CI, $n = 7$). Each data point represents the average modulus of ≥ 10 indentation locations from one animal. **c)** Schematic illustration of perlecan IF-guided AFM-nanomechanical mapping experimental set-up and a representative 15 μm × 20 μm map of indentation modulus, E_{ind}, measured from 3-month-old wild-type condylar cartilage, which illustrates the separation of the PCM and T/IT-ECM microdomains in the hyaline layer. **d)** Box-and-whisker plot of E_{ind} distribution on the PCM (≥ 600 locations from $n \geq 5$ animals for each genotype) and T/IT-ECM (≥ 2,800 locations, $n \geq 5$) of the hyaline layer (*p*-values were obtained via Mann-Whitney test on the averaged modulus from each animal). Each data point represents the average value measured from one animal.

Figure 5 Impact of induced collagen V knockout on the post-natal growth of TMJ condylar cartilage. **a)** Quantitative PCR (qPCR) on the condylar cartilage between wild-type (WT), *Col5a1*$^{f/f}$*/Rosa26Cre*^{ER} mice injected with vehicle (V) or tamoxifen (TM) at 1 month of age illustrates the reduction of *Col5a1* gene by TM (mean ± 95% CI, $n = 6$). **b)** Immunofluorescence (IF) images of collagen V show the reduction of collagen V protein after the induced knockout (*iKO*) of *Col5a1* gene at 1 month (TM injection at 1 week of age) and 2 months (TM injection at

1 month) of ages, respectively (F: fibrous layer, H: hyaline layer). **c)** Safranin-O/Fast Green histology images illustrate the absence of morphological changes at 1 month of age, but a substantial reduction in the hyaline layer thickness at 2 months of age (black arrowheads), after the induced knockout of *Col5a1* gene. **d)** Cartilage thickness, **e)** cellular density, **f)** cell arrangement score on each of the fibrous (F) and hyaline (H) layer, and **g)** indentation modulus, E_{ind}, measured on condylar cartilage surface following the induced knockout of collagen V ($n \geq 5$, mean ± 95% CI, *: $p < 0.05$). Each data point represents the average value measured from one animal.

Figure 6 Absence of gross-level knee cartilage morphological phenotype with the reduction of collagen V. **a)** Immunofluorescence (IF) images of collagen V show the presence of minor amount of collagen V on the superficial layer of knee cartilage in wild-type (+/+) and *Col5a1*$^{+/-}$ (+/−) mice at 3 months of age. **b)** Hematoxylin and Eosin (H&E, top panel) and Safranin-O/Fast Green (bottom panel) histology images of knee cartilage. *Col5a1*$^{+/-}$ knee cartilage shows no appreciable changes in cartilage morphology, sulfated glycosaminoglycan (sGAG) staining, cell density or arrangement. **c)** Uncalcified and total cartilage thickness, **d)** cellular density within each of the uncalcified and calcified cartilage layer of knee cartilage at 3 months of age ($n = 5$, mean ± 95% CI). Each data point represents the average value measured from one animal.

Figure 7 Impact of collagen V reduction on the surface collagen fibril nanostructure and biomechanical properties of knee cartilage. **a)** Representative electron microscopy images of collagen fibril nanostructure of wild-type (+/+) and *Col5a1*$^{+/-}$ (+/−) murine knee cartilage surface at 3 months of age via SEM. **b)** Histogram of fibril diameter distribution, d_{col} (≥ 420 fibrils from $n = 4$ animals for each genotype). Shown together are the normal distribution, $N(\mu, \sigma^2)$, fits to fibril diameters (for each fit, values of μ and σ correspond to the mean and standard deviation of fibril diameters; $p = 0.848$ between the two genotypes via unpaired two-sample *t*-test). **c)** Comparison of fibril diameter heterogeneity (variance) between the two genotypes (mean ± 95% CI). **d)** AFM-nanoindentation modulus, E_{ind}, of murine knee cartilage surface at 3 months of age ($n \geq 6$. mean ± 95% CI). Each data point represents the average value measured from one animal.

Figure 8 Absence of structural or biomechanical defects in knee cartilage with the induced knockout of collagen V. **a)** Safranin-O/Fast Green histology images of control and induced collagen V knockout (*iKO*) murine knee cartilage at 1 month (TM injection at 1 week) and 2 months (TM injection at 1 month) of ages. Both age groups show no appreciable changes in cartilage morphology, sulfated glycosaminoglycan (sGAG) staining, cell density or arrangement. **c)** Uncalcified and total cartilage thickness, **d)** cellular density within each of the uncalcified and calcified cartilage layer, and **e)** AFM-nanoindentation modulus, E_{ind}, of murine knee cartilage surface following the induced knockout of collagen V ($n \geq 5$, mean ± 95% CI). Each data point represents the average value measured from one animal.

Figure 9 Reduction of cell proliferation and β-catenin expression in the fibrous layer cells of condylar cartilage after the induced knockout of collagen V. a) Immunofluorescence (IF) images show appreciable staining of Ki-67 in the fibrous layer of condylar cartilage in control mice, and its reduction in that of induced collagen V knockout (*iKO*) mice at 1 month of age (TM injection at 1 week of age). Knee cartilage in either control or *iKO* mice does not show appreciable Ki-67 staining. b) Comparison of the percentage of Ki-67 positive cells in TMJ condylar cartilage fibrous layer between control and *iKO* mice. c) IF images show the appreciable staining of β-catenin in the fibrous layer cells of condylar cartilage in control mice, and its reduction in that of

iKO mice. Knee cartilage in both genotypes does not show appreciable β-catenin staining. d) Comparison of relative β-catenin intensity normalized by DAPI number in condylar cartilage fibrous layer between control and *iKO* mice. e) Zoom-in β-catenin IF images illustrate the presence of β-catenin nuclear translocation in both control and *iKO* mice (white arrowheads).

Figure 10 Schematic illustration of the working hypothesis on the role of collagen V in TMJ condylar cartilage ECM, inspired by Refs. [44, 47]. In the condylar cartilage, collagen V regulates the assembly of collagen I fibrils, and thus, determines the integrity and mechanical properties of the fibrous layer. In addition, collagen V also mediates the mechanobiology of progenitor cells in the fibrous layer, and in turn, regulates the proliferation, mechanosensing and Wnt/β-catenin signaling of these cells. Given that these progenitors undergo chondrogenesis and give rise to hyaline cartilage during post-natal growth [46, 47], collagen V thus plays a crucial role in regulating the development of the secondary hyaline layer.

Tables

Table 1 Summary of collagen fibril diameter distributions on the surface, in the interior fibrous and hyaline layers of TMJ condylar cartilage, as well as the surface of knee cartilage, measured by scanning electron microscopy (SEM) and transmission electron microscopy (TEM)

unit (nm)	TMJ Condylar Cartilage						Knee Cartilage	
	Surface		Fibrous Layer		Hyaline Layer		Surface	
	+/+	+/–	+/+	+/–	+/+	+/–	+/+	+/–
mean	25	31	21	34	24	33	33	33
std	5	7	7	10	6	9	7	13
Q_1	21	26	17	28	20	27	29	22
Q_2	24	31	20	32	23	33	32	30
Q_3	28	36	25	38	27	39	36	41
min	11	16	8	13	11	15	16	11
max	48	63	50	85	50	71	68	77
n_{fibrils}	812	887	485	362	553	585	420	509
adjusted p-value (mean)	< 0.0001		< 0.0001		< 0.0001		0.848	
adjusted p-value (variance)	< 0.0001		< 0.0001		< 0.0001		< 0.0001	

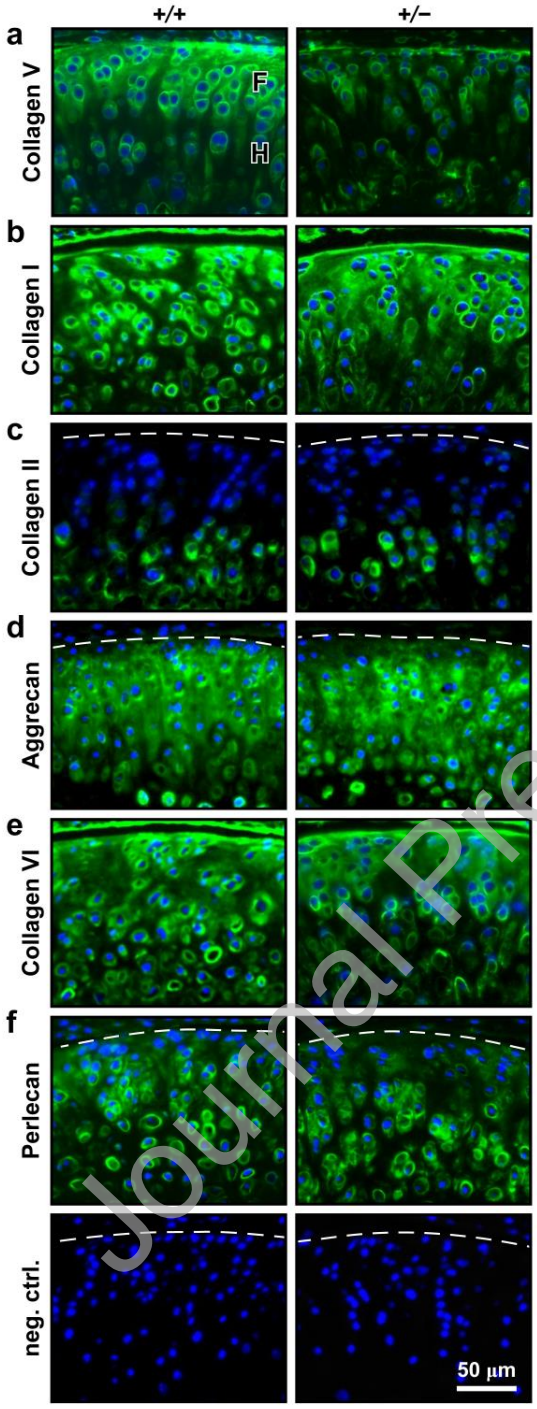

Fig. 1

Fig. 2

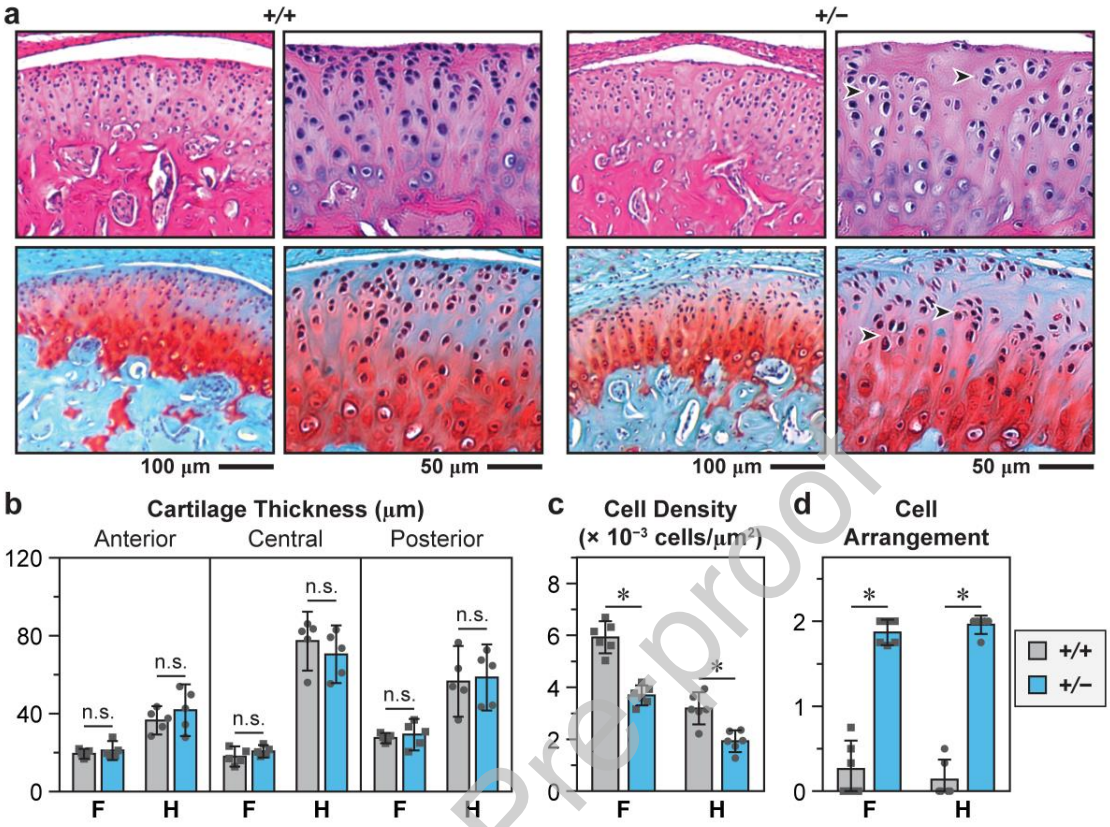

Fig. 3

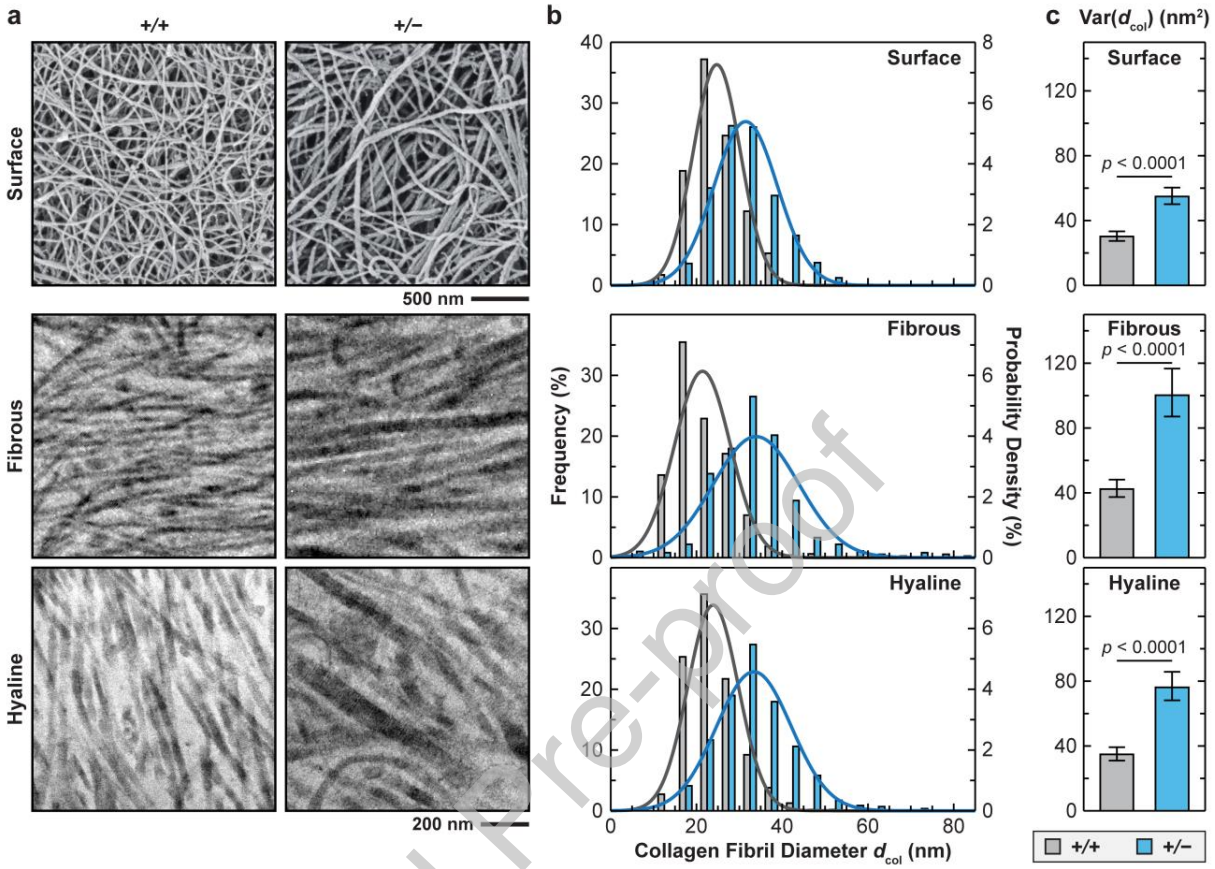

Fig. 4

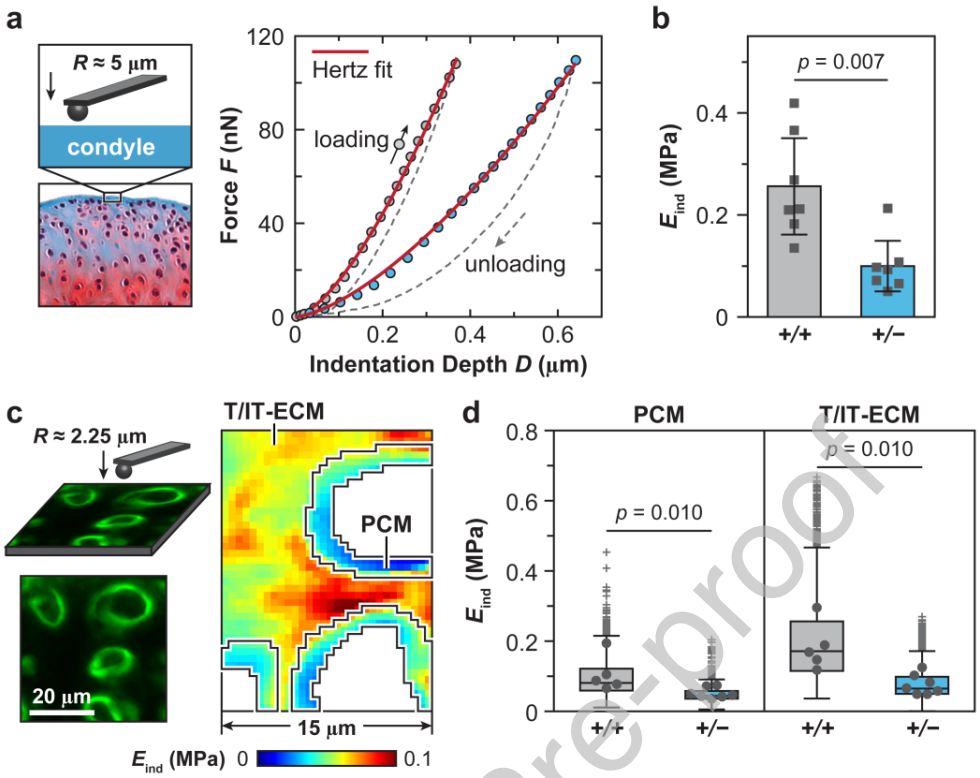

Fig. 5

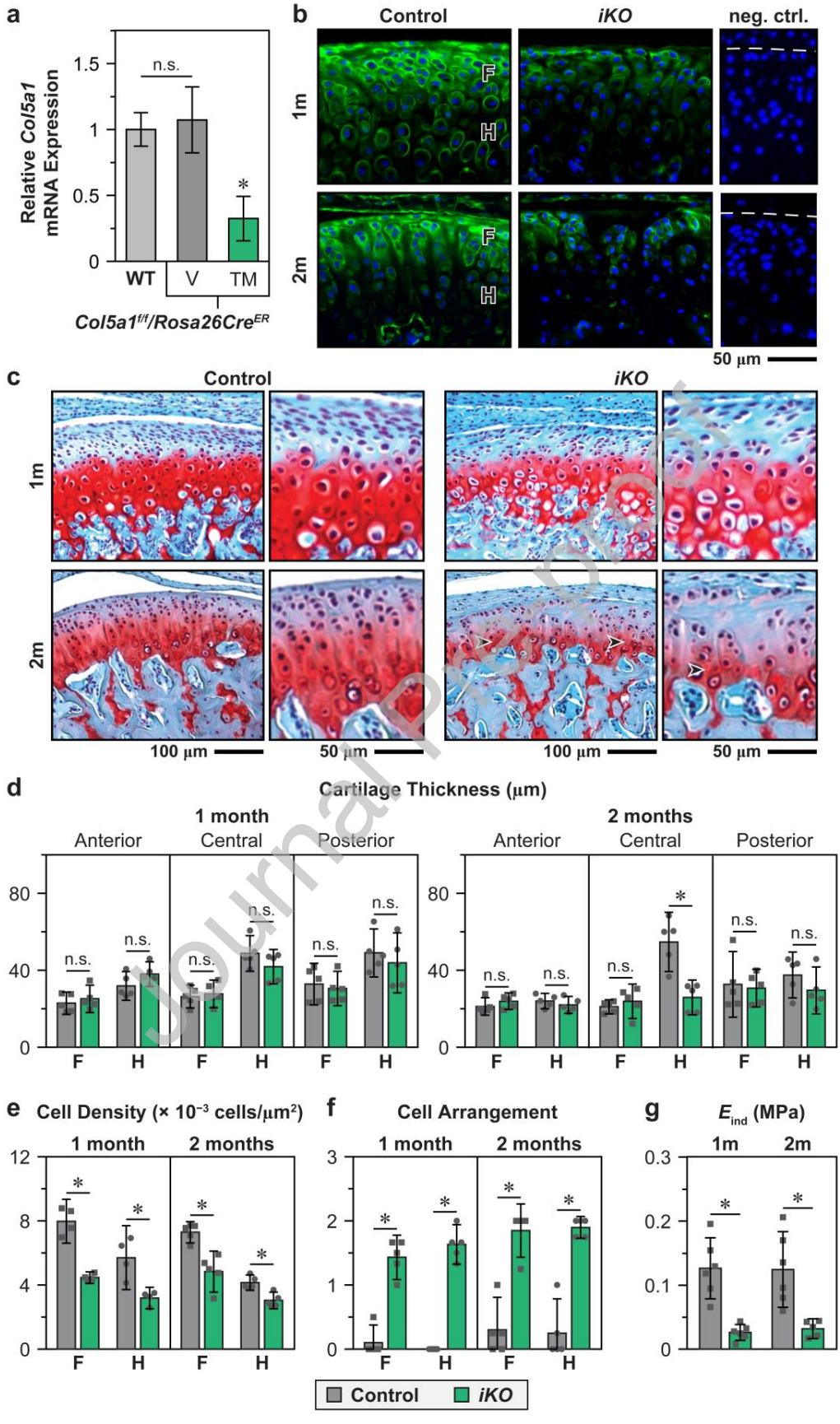

Fig. 6

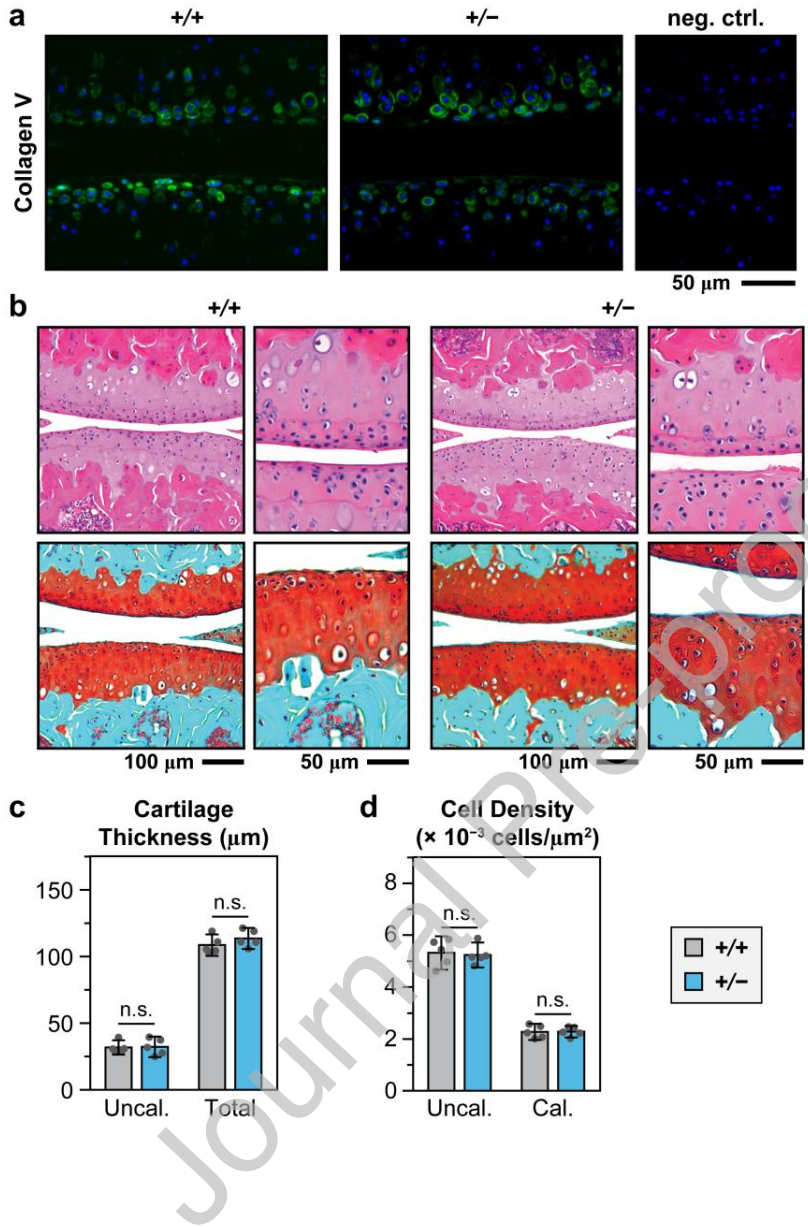

Fig. 7

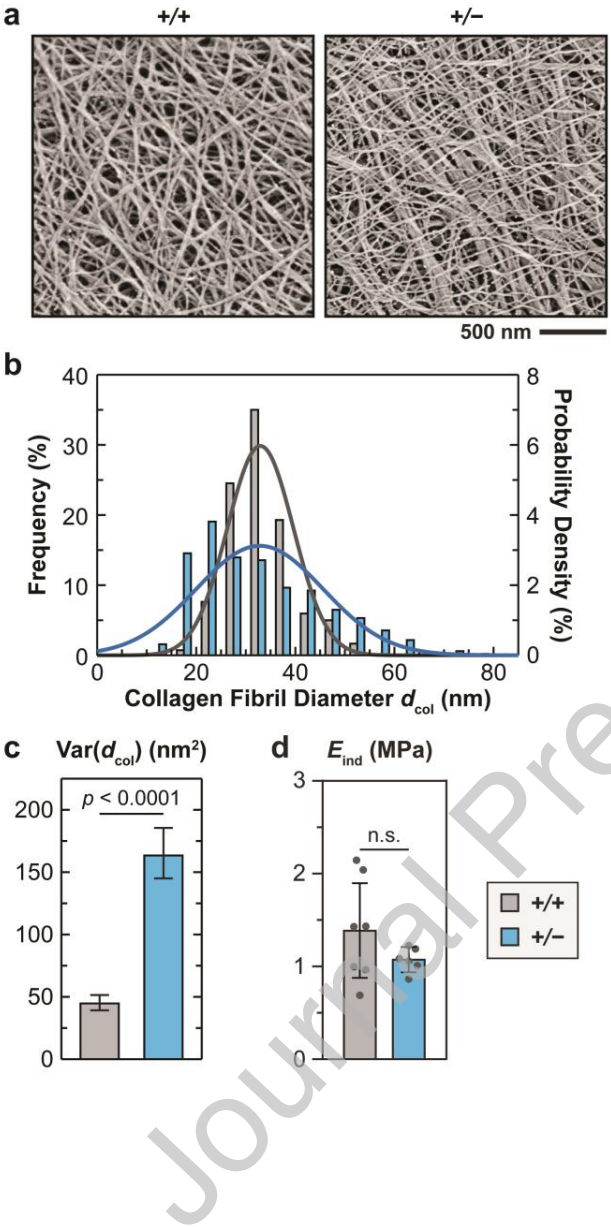

Fig. 8

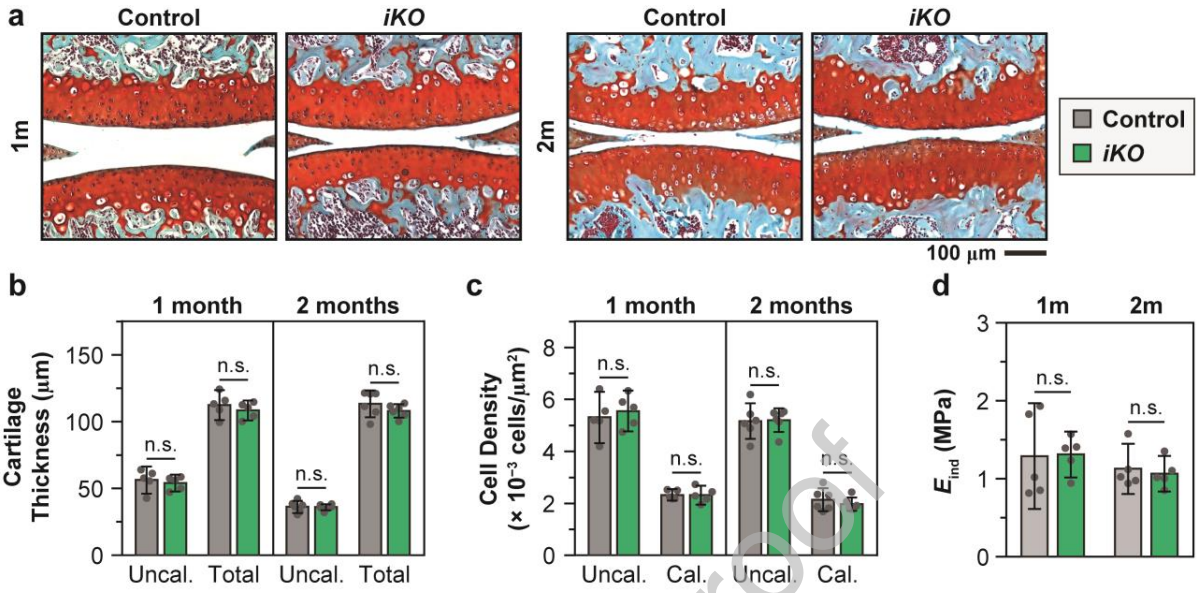

Fig. 9

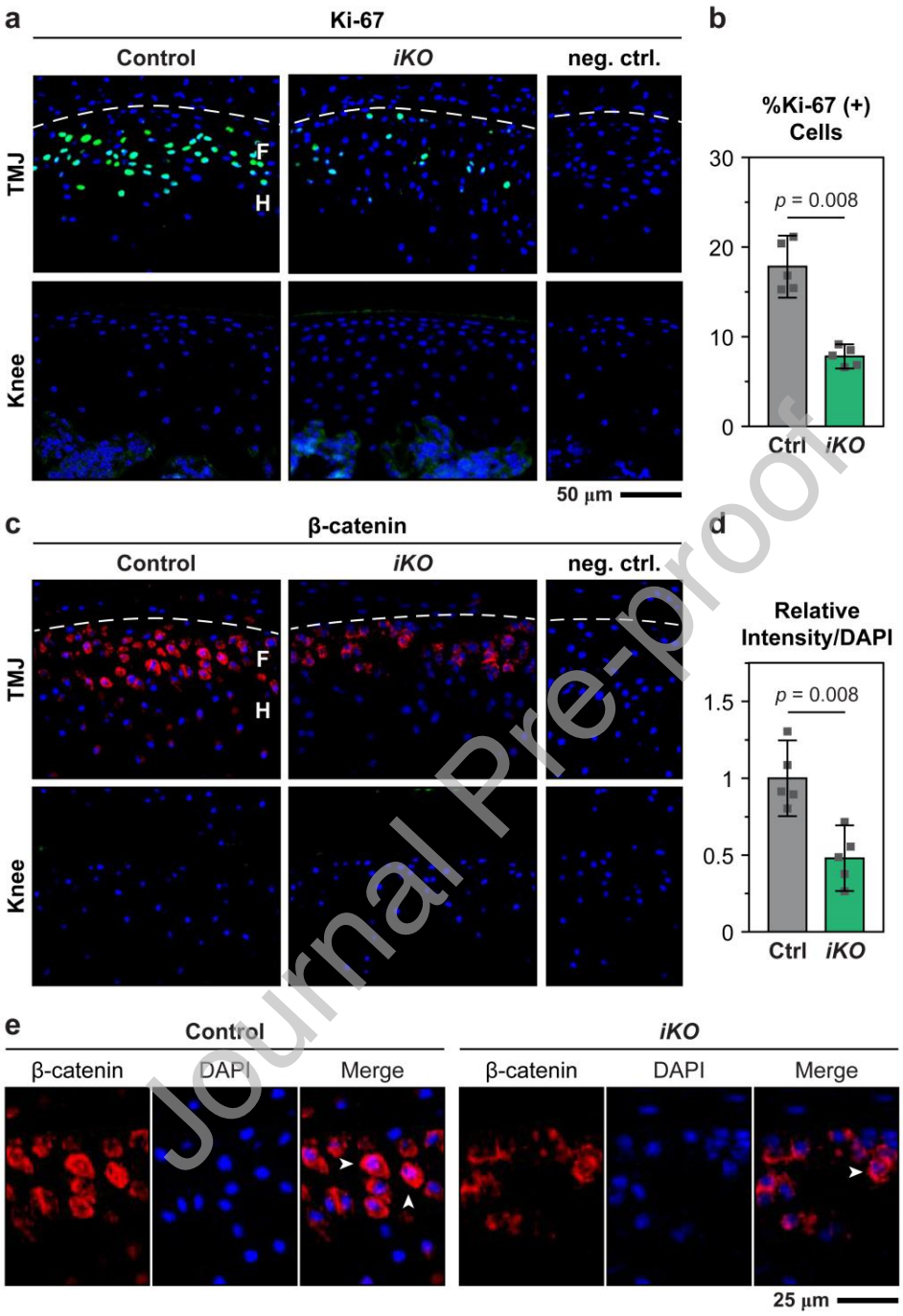

Fig. 10